

# Behavior of optimized prestressed concrete composite box-girders with corrugated steel webs

Yanqiu Lu <sup>\*1,2</sup> and Lun Ji <sup>3</sup>

<sup>1</sup> Beijing Capital Highway Development Group Co., Ltd, Beijing, China

<sup>2</sup> Department of Civil Engineering, Tsinghua University, Beijing, China

<sup>3</sup> School of transportation science and engineering, Harbin Institute of Technology, Harbin, China

(Received May 17, 2017, Revised December 5, 2017, Accepted December 5, 2017)

**Abstract.** The traditional prestressed concrete composite box-girders with corrugated steel webs have several drawbacks such as large deflection and potential local buckling. In this study, two methods were investigated to optimize and improve the prestressed concrete composite box-girders with corrugated steel webs. The first method was to replace the concrete bottom slab with a steel plate and the second method was to support the concrete bottom slab on the steel flanges. The behavior of the prestressed concrete composite box-girders with corrugated steel webs with either method was studied by experiments on three specimens. The test results showed that behavior of the optimized and upgraded prestressed concrete composite box-girders with corrugated steel webs, including ultimate bearing capacity, flexural stiffness, and crack resistance, is greatly improved. In addition, the influence of different shear connectors, including perfobond leisten (PBL) and stud shear connectors, on the behavior of prestressed concrete composite box-girders with corrugated steel webs was studied. The results showed that PBL shear connectors can greatly improve the ultimate bearing capacity, flexural stiffness and crack resistance property of the prestressed concrete composite box-girders with corrugated steel webs. However, for the efficiency of prestressing introduced into the girder, the PBL shear connectors do not perform as well as the stud shear connectors.

**Keywords:** corrugated steel webs; steel flanges; efficiency of prestressing introduced; studs shear connectors; PBL; ultimate bearing capacities; flexural stiffness; crack resistance property

## 1. Introduction

The first prestressed concrete composite box-girders bridge with corrugated steel webs in the world, the Coganc Bridge, was built in 1986 in France (He *et al.* 2014, Li *et al.* 2012). After the Coganc Bridge was successfully finished, this type of bridge was widely constructed in the world. For example, in France, the Maupre Bridge and the Dole Bridge were respectively built in 1987 (Ding *et al.* 2012) and in 1993 (Kim *et al.* 2011). In Japan, the Maetani Bridge was built in 2001 (Yong *et al.* 2013). In German, the Altwipfergrund Bridge was built in 2001, which is first the type of bridge in German (Ahn *et al.* 2010). The Pohe Bridge, in China, was built in 2005 (Huang and Chen 2016). The Ilsun Bridge was constructed in South Korea, which was the world's longest (801 m in total length) and widest (30.9 m in maximum width) prestressed concrete composite box girder bridge with corrugated steel webs by 2008 (Jung *et al.* 2011). The diagrammatic sketch of the prestressed concrete box-girders with corrugated steel webs is shown in Fig. 1. The traditional prestressed concrete composite box-girders bridge with corrugated steel web has some attractive advantages (The cross-section of the traditional prestressed concrete composite box-girders with

corrugated steel is shown in Fig. 2(a). Firstly, the corrugated webs can improve the efficiency of prestressing introduced into the top/bottom slabs through the accordion effect that occurs due to the low axial stiffness of the corrugated webs when the prestressing is introduced (He *et al.* 2012). Secondly, because the corrugated steel webs replaced the concrete webs, the dead weight is decreased, and this leads to reduce seismic forces. Furthermore, the decreasing dead weight also leads to the smaller substructures, which will cut down the cost of the bridge (Sause *et al.* 2015). Thirdly, the use of corrugated webs can also avoid some of the cracks on the concrete webs (Nie *et al.* 2012). In addition, the prestressed concrete composite girders with corrugated steel webs can be advantageous for beam height reduction (Basher *et al.* 2011).

Although the above mentioned advantages are attractive, there are some disadvantages on the traditional prestressed concrete composite box-girders bridge with corrugated steel webs. Firstly, after the traditional prestressed concrete composite box-girders bridge with corrugated steel webs was used for a period of time, the mid-span deflection of box-girders was increased significantly, and even exceeded the limited value which was set in specification (Huang and Chen 2016, Barakat *et al.* 2015). Secondly, compared to the steel flanges located below the concrete bottom slab (as shown in Fig. 2(b)), the steel flanges located on the concrete bottom slab (as shown in Fig. 2(a)) are not efficiently worked. The reason is that the steel flanges located on the

\*Corresponding author, Ph.D. Student,  
E-mail: [luyanqiu2008@126.com](mailto:luyanqiu2008@126.com)

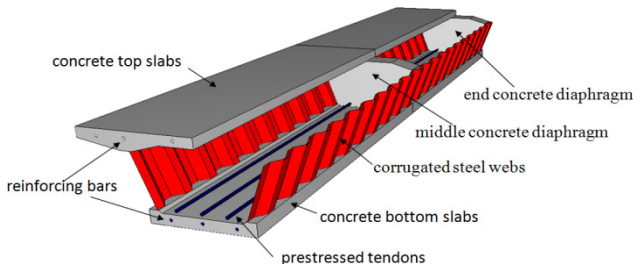
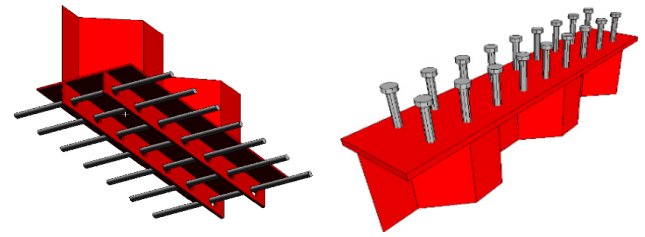


Fig. 1 Schematic diagram of prestressed concrete composite box-girders with corrugated steel webs

concrete bottom cause the distance  $X_1$  (between neutral axial and steel flanges) to be smaller than the distance  $X_2$  (between neutral axial and steel flanges). Thirdly, the concrete bottom slab is hung below the corrugated steel webs welded with the steel flanges (as shown in Fig. 2(a)), this can cause that the concrete bottom slab has a potential tendency to drop off from the corrugated steel webs.

To solve these drawbacks, the traditional prestressed concrete composite box-girders with corrugated steel webs was optimized and upgraded by two ways. The first method was to replace the concrete bottom slab with a steel plate (as shown in Fig. 2(c)) and the second method was to support the concrete bottom slab on the steel flanges (as shown in Fig. 2(b)).

In addition, the shear connectors used to bond with the concrete top/bottom slab and corrugated steel webs are one of the key factors that ensures the prestressed concrete composite box-girders with corrugated steel webs normal works (Song *et al.* 2014). At present, two types of shear



(a) PBL shear connectors (b) Stud shear connectors

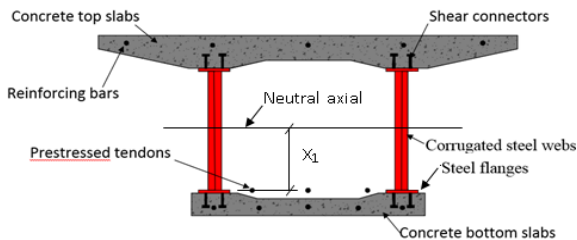
Fig. 3 Shear connectors

connectors, perfobond leisten (PBL) shear connectors and stud shear connectors (as shown in Fig. 3), are widely used on the prestressed concrete composite box-girders bridge with corrugated steel webs (Lee *et al.* 2015). The two shear connectors may differently affect behavior of the prestressed concrete composite box-girders with corrugated steel. So the two types of shear connectors, PBL and studs, were studied by the test methods in the study.

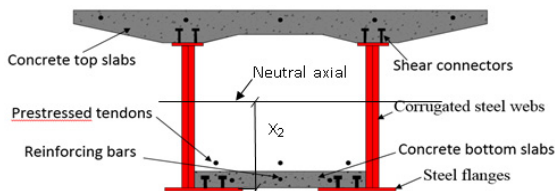
## 2. Test program

### 2.1 Specimens

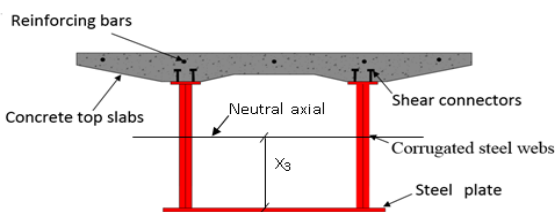
Table 1 shows the summary of test specimens studied in this paper, among which three prestressed concrete composite girders with corrugated webs, named BXL-A, BXL-C, and BXL-D, were tested to assess their flexural behavior. In addition, the prestressed concrete composite



(a) Traditional prestressed concrete composite box-girders with corrugated steel



(b) Upgraded prestressed concrete composite box-girders with corrugated steel



(c) Upgraded prestressed concrete composite box-girders with corrugated steel

Fig. 2 Traditional and upgraded prestressed concrete composite box-girders with corrugated steel

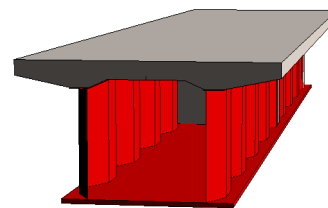
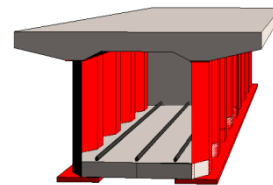
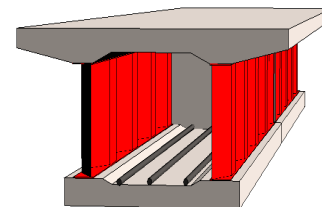


Table 1 Test specimens

Specimens	Position of concrete bottom slab	Type of shear connectors	Prestressed tendons	Usage or purpose
BXL-A	hung below corrugated steel webs	studs	yes	A* and B*
BXL-B	hung below corrugated steel webs	PBL	yes	A*
BXL-C	supported on corrugated steel webs	studs	yes	B*
BXL-D	no	studs	no	B*

\*A: By comparing specimens BXL-A and BXL-B, researching on impact of different shear connectors on behavior of the prestressed concrete composite box-girders with corrugated steel

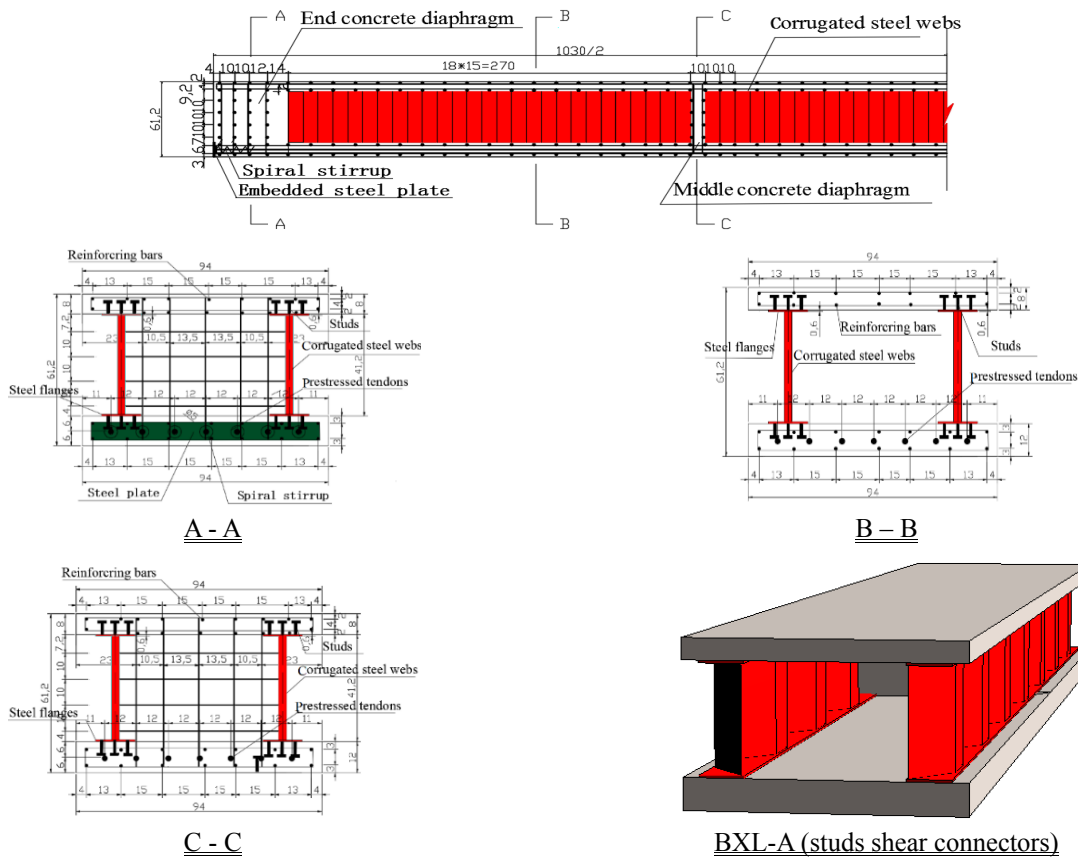
\*B: By comparing specimens BXL-A, BXL-C and BXL-D, researching on behavior of the optimized and upgraded prestressed concrete composite box-girders with corrugated steel webs

girder with corrugated webs, named BXL-B, was tested to evaluate the impact of a different type of shear connectors on structure performances.

Fig. 4 shows the specimen profiles, dimensions, and sectional details of each specimen. The BXL-A specimen was the traditional prestressed concrete composite box-girders with corrugated steel webs (as shown in Fig. 4(a)), whose concrete bottom slab was hung below the flange, with studs shear connectors. The BXL-B specimen whose concrete bottom slab was hung below the flange, with PBL shear connectors, was also the traditional prestressed concrete composite box-girders with corrugated steel webs (as shown in Fig. 4(b)). The two specimen were used to study the impact of the different shear connectors on the

structure performances. The BXL-C specimen was the optimized and upgraded type of prestressed concrete composite box-girders with corrugated steel webs (as shown in Fig. 4(c)), whose concrete bottom slab was supported on the flanges, with studs shear connectors. The BXL-D specimen, with studs shear connectors, was also the optimized and upgraded type of prestressed concrete composite box-girders with corrugated steel webs (as shown in Fig. 4(d)), whose concrete bottom slab was replaced by a steel plate and the prestressed tendons were not used.

All of the specimens were 10300 mm long and 612 mm high. Both of end concrete diaphragms were 500 mm thick, and there were two middle concrete diaphragms of 100 mm



(a) BXL-A

Fig. 4 Sections of Specimens BXL-A, BXL-B, BXL-C, BXL-D (unit: cm)

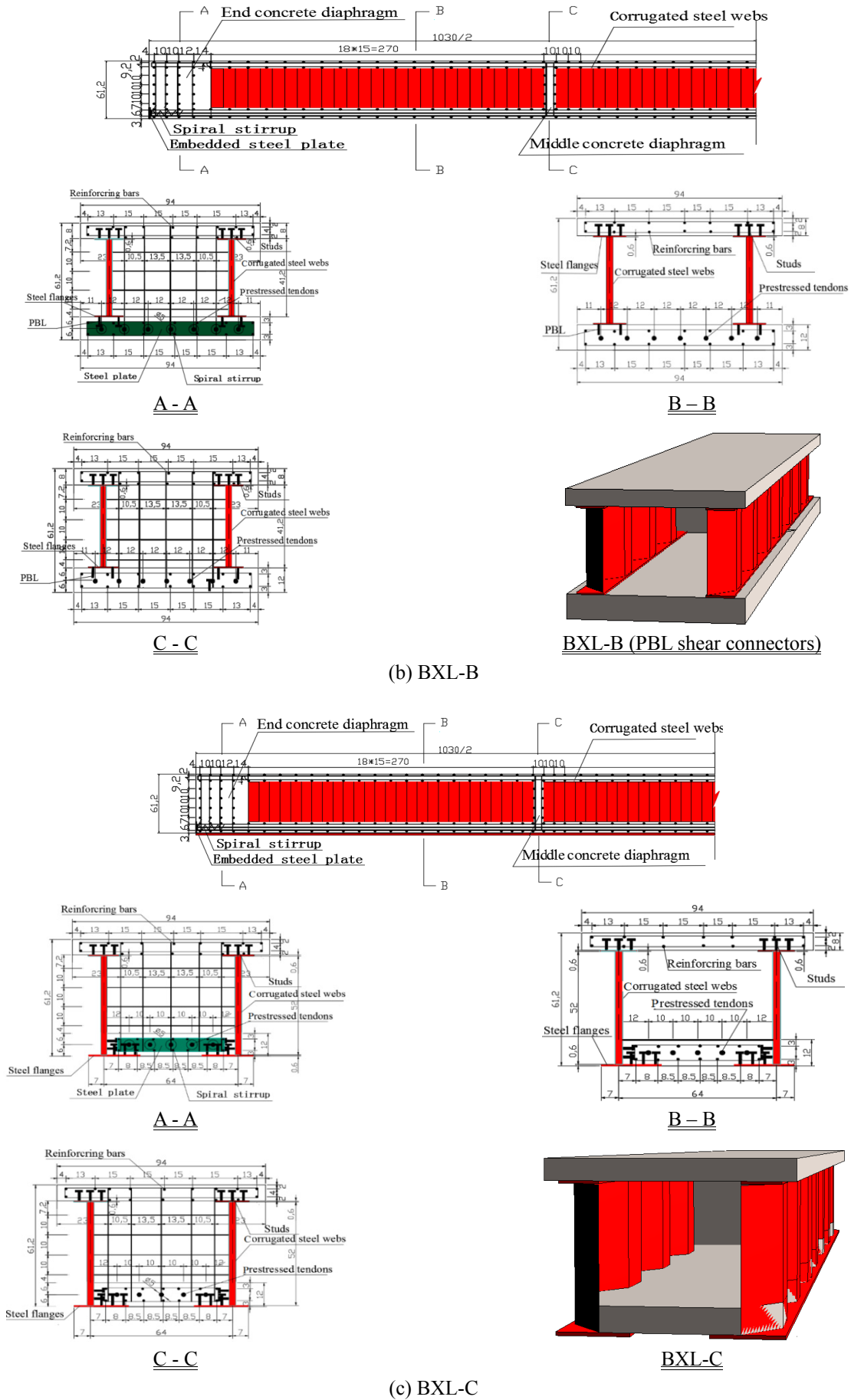
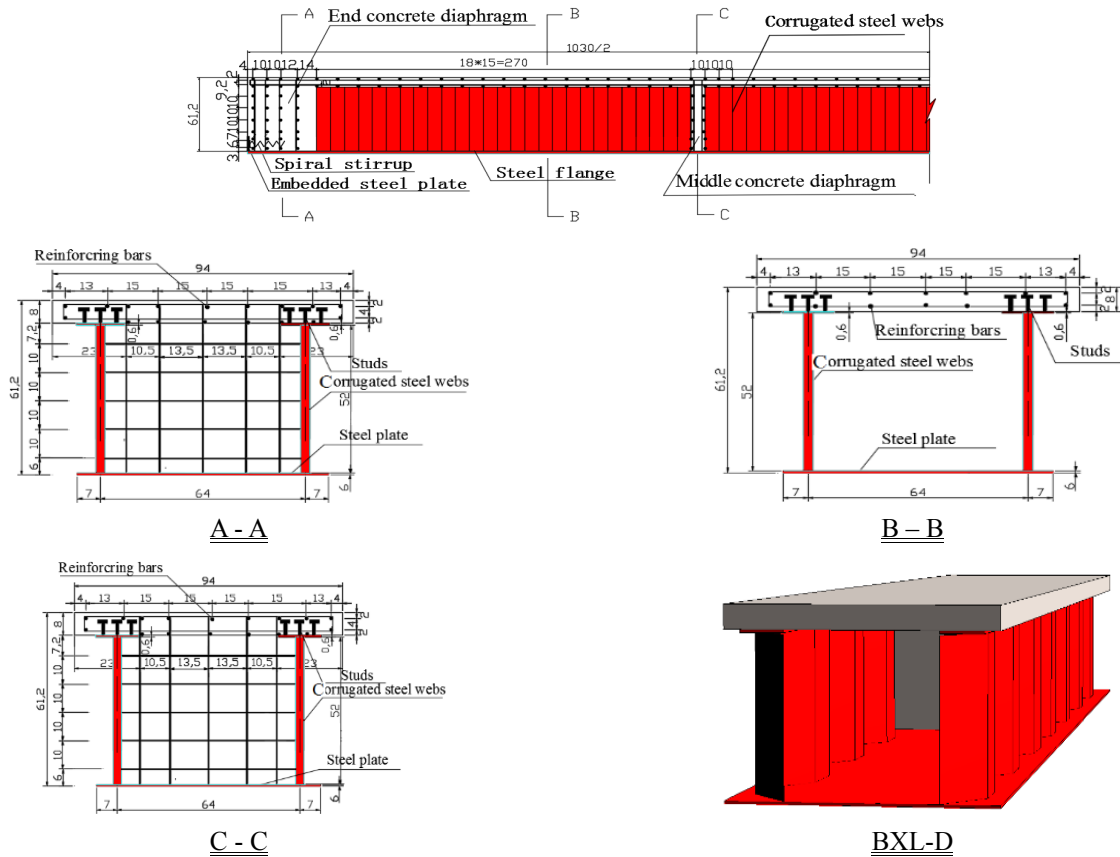


Fig. 4 Continued



(d) BXL-D

Fig. 4 Continued

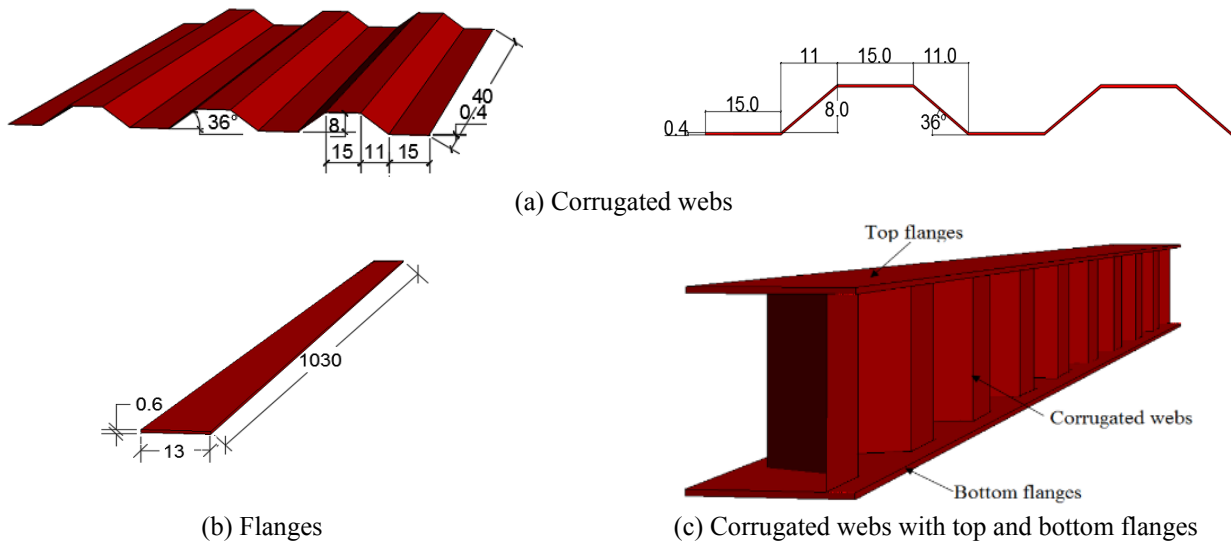


Fig. 5 Dimensions of corrugated webs and top/bottom flanges (unit: cm)

thickness, which were 3200 mm from each end of the specimen. The concrete top and bottom slab were 80 mm and 120 mm thick, respectively.

The corrugated webs of specimens BXL-A and BXL-B were 400 mm high, and that of specimens BXL-C and BXL-D were 520 mm high. All of the corrugated webs were 4 mm thick. All of the top/bottom flanges were 6 mm thick and 130 mm width. The bottom steel plate of the BXL-D

specimen was also 6 mm thick. All corrugated webs were manufactured with an 80 mm wave height and a 36° wave height angle, and no extra stiffener was installed in the web. The dimensions of corrugated webs and the top/bottom flanges are showed in Fig. 5.

As shown in Fig. 6, after the top/bottom flanges and the corrugated webs were manufactured separately, they were welded together.

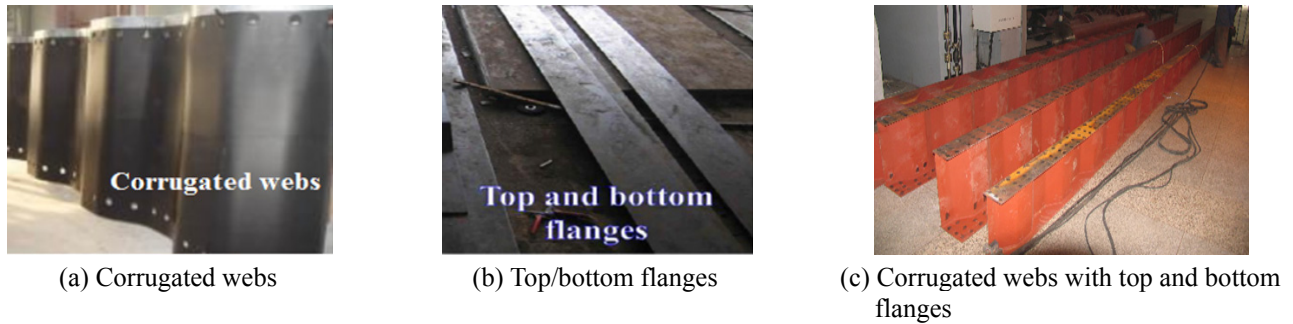


Fig. 6 Corrugated webs ,flanges, and corrugated web with top and bottom flanges

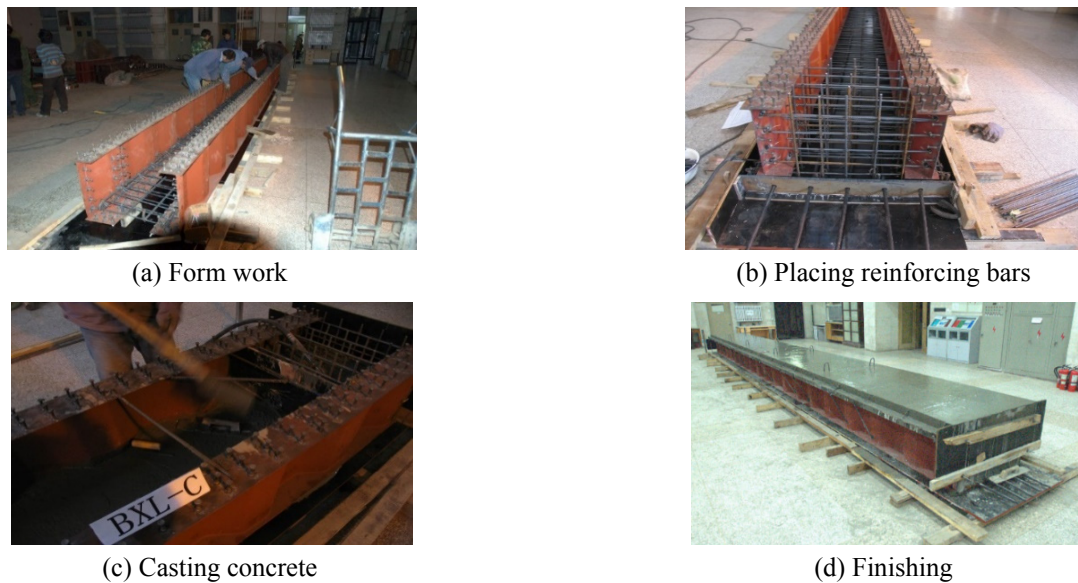


Fig. 7 Fabrication of the specimens

After forms were set on the sides of the box-girders, the slab reinforcing bars were placed, and concrete was cast in place, as shown in Figs. 7(a) to (d).

Shear studs with a 440 MPa tensile strength and a 10 mm diameter with a 20 mm stud head diameter were placed at 100 mm spacing on steel flanges.

As shown in Fig. 4, the composite sections of all specimens BXL-A, BXL-B, BXL-C and BXL-D are box-shaped, and the concrete top slab was 80 mm thick and 940 mm wide. The height of the composite section was 612 mm. In the concrete top slabs, D16 longitudinal reinforcing bars were placed at 130 mm or 150 mm spacing in double layers, and D13 bars were also placed in perpendicular direction at 500 mm spacing in double layers. The tendons, 15.2 mm

diameter, were placed at 120 mm spacing in the concrete bottom slab. The concrete mix proportion is shown in Table

Table 2 Concrete mixture proportion

Mix strength (MPa)	$G_{max}$ * (mm)	W/C* (%)	S/A* (%)	Unit volume weight (kg/m <sup>3</sup> )				
				W*	C*	S*	G*	AD*
50	30	42.3	45.5	160	369	825	975	1.85

\* $G_{max}$ : maximum aggregate size, \*W/C: water to cement ratio,

\*S/A: fine aggregate ratio, \*W: water, \*C: cement,

\*S: fine aggregate, \*G: coarse aggregate, and

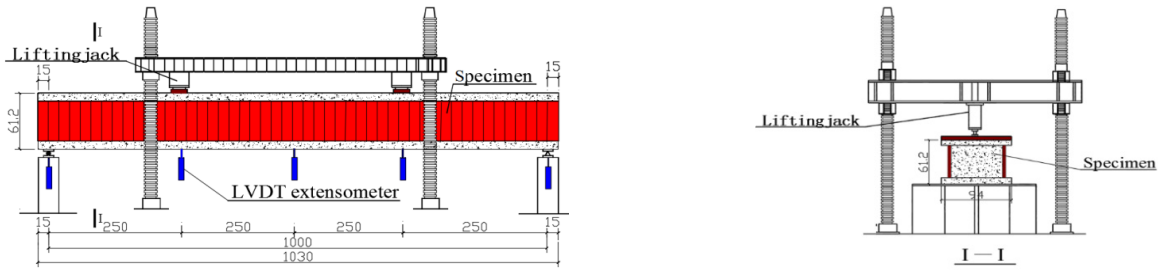
\*AD: air entraining water reducing agent

Table 3 Material test results

Specimens	Reinforcement				Tendon
	D13		D16		$\phi 15.2$
	$E_s$ (MPa)	$f_y$ (MPa)	$E_s$ (MPa)	$f_y$ (MPa)	$E_{pu}$ (MPa)
BXL-A	$2.0 \times 10^5$	410	$2.0 \times 10^5$	410	1855
BXL-B	$2.0 \times 10^5$	410	$2.0 \times 10^5$	410	1855
BXL-C	$2.0 \times 10^5$	410	$2.0 \times 10^5$	410	1855
BXL-D	$2.0 \times 10^5$	410	$2.0 \times 10^5$	410	1855

Specimens	Steel				Concrete
	Thickness 4 mm		Thickness 6 mm		Compressive strength
	$E_s$ (MPa)	$f_y$ (MPa)	$E_s$ (MPa)	$f_y$ (MPa)	$f_c$ (MPa)
BXL-A	$2.0 \times 10^5$	270	$2.0 \times 10^5$	220	55
BXL-B	$2.0 \times 10^5$	270	$2.0 \times 10^5$	220	55
BXL-C	$1.9 \times 10^5$	290	$2.0 \times 10^5$	292	50
BXL-D	$1.9 \times 10^5$	290	$2.0 \times 10^5$	292	50

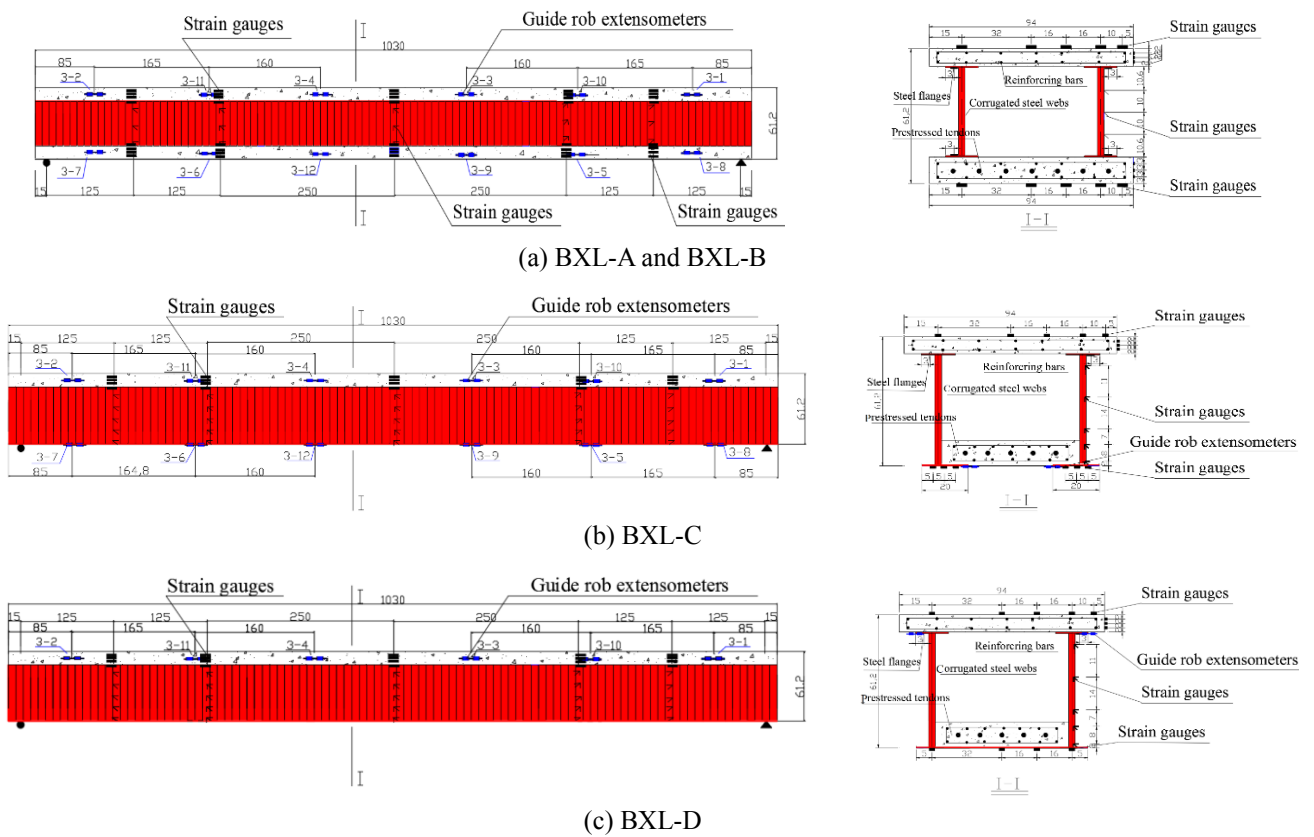


(a) Location of LVDT extensometers and dimensions of loading geometry (unit: cm)



(b) Photo of loading device

Fig. 8 Loading device



(a) BXL-A and BXL-B

(b) BXL-C

(c) BXL-D

Fig. 9 Location of guide rod extensometers and strain gauges (unit: cm)

2, and material test results on concrete, reinforcing bars, tendons, and steel plates are presented in Table 3.

### 2.2 Loading and measurements

As shown in Fig. 8, the specimens were simply supported with a span length of 1000 cm. Their deflections

were measured by five LVDT extensometers installed under the specimens, which were located at the two end supports, the two point concentrated load, and the center of the specimens.

The relative slip between the steel flange and the concrete top/bottom slabs during the loading history was monitored by the guide rod extensometers installed at both



Fig. 10 Test process of BXL-C specimen

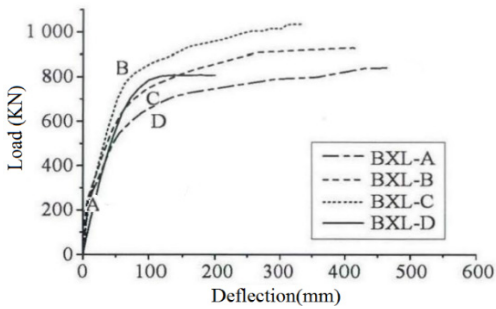


Fig.11 Load-deflection curves

ends of the members, as shown in Fig. 9. The strains in the longitudinal direction of the specimens were measured by the strain gauges attached on the surface of the concrete top and bottom slab, the top and bottom flanges and the corrugated webs, as shown in Fig. 9.

### 3. Test process

The same design prestressing, which was 3.0 MPa, was introduced into the concrete bottom slab of the specimens BXL-A, BXL-B and BXL-C (the prestressed tendons were

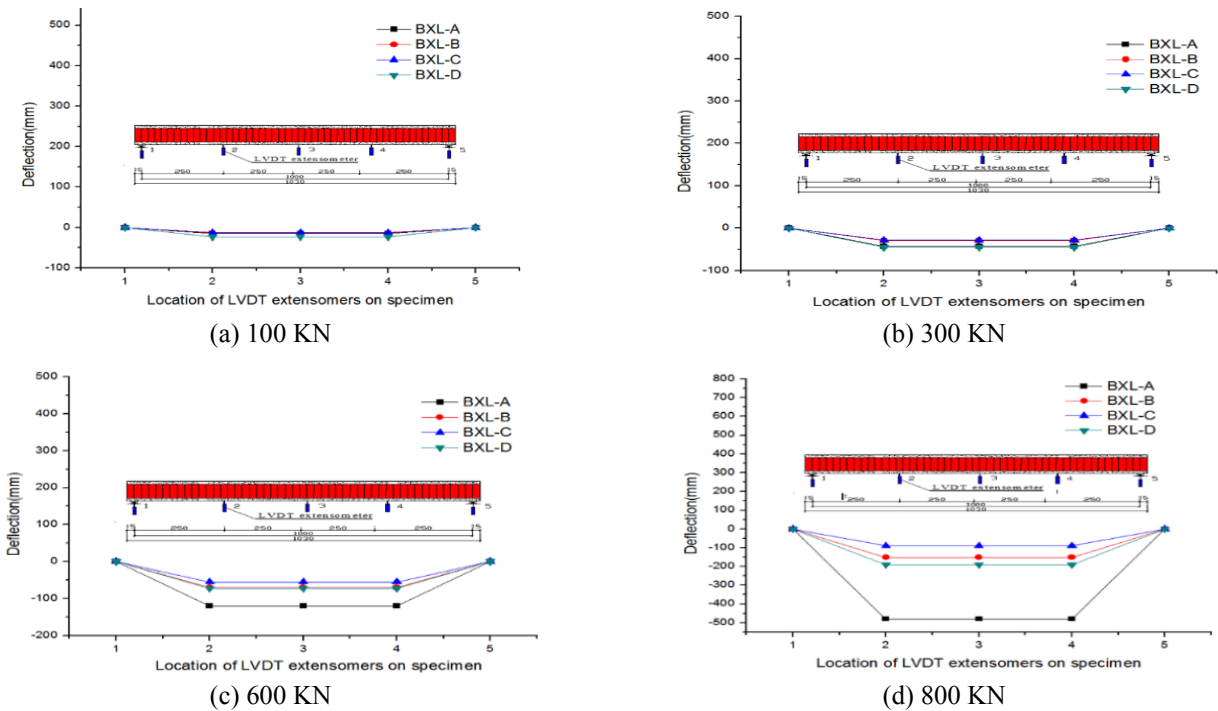


Fig. 12 Deflections of specimens

not utilized on the BXL-D specimen). To ensure that the prestressing was evenly distributed along the tendon, the prestressing was introduced twice into specimens, and the half of the prestressing (approximately 1.5 MPa) was introduced every time. After the first stage was finished, there was a five minutes break, and then the second stage of prestressing was introduced up to the target prestressing, which was 3.0 MPa. The targeted prestressing was effective prestressing considering the instantaneous loss caused by the anchorage seating and the elastic shortening.

The composite girder was fixed on an experimental bench. A two point concentrated load was applied on the specimen under the displacement control and the loading was initiated. Fig. 10 shows the test process of the BXL-C specimen.

## 4. Test analyses

### 4.1 Behavior of the prestressed concrete composite box-girders with corrugated webs

#### 4.1.1 The load–displacement responses of test specimens

Fig. 11 shows the load-displacement responses of test specimens. Except for the BXL-D specimen, the specimens BXL-A, BXL-B, and BXL-C showed almost similar load-deflection behaviors to each other up to a maximum load. Their loads-displacement curves were continually increased with two obvious turning points A and B(C, D). The turning points A indicated that the concrete bottom slab had cracked, and the turning points B(C, D) indicated that the tension reinforcement in the concrete bottom slab had yielded. Therefore, the specimens BXL-A, BXL-B, and BXL-C showed the perfect nonlinear behavior in the overall loading history.

The behavior of the BXL-D specimen was different from the specimens BXL-A, BXL-B, and BXL-C. Before reaching a maximum load, the load - displacement curve of the BXL-D specimen showed linear behavior without any turning point.

#### 4.1.2 Ultimate bearing capacities in prestressed concrete composite box-girders with corrugated steel webs

The ultimate load of the BXL-C specimen, which was 1034 KN, was the largest; the ultimate load of the BXL-B specimen, which was 930 KN, was second. The ultimate loads values of the specimens BXL-A and BXL-D, which were 822 KN and 818 KN, respectively, were similar and were the smallest. Compared to the BXL-A specimen, the ultimate bearing capacities of the BXL-C specimen was increased by 25.79%. Therefore, the conclusion can be drawn that the ultimate bearing capacities of the prestressed concrete composite box-girders with corrugated steel webs which was optimized and upgraded by the method that the concrete bottom slab was supported on the steel flanges could observably be improved.

#### 4.1.3 Flexural stiffness in prestressed concrete composite with corrugated steel webs

Fig. 11 showed that before the test specimens' crack occurred, the initial flexural stiffness, in the specimens BXL-A, BXL-B, and BXL-C, were the similar, and the BXL-D specimen was smaller than the other three specimens. But after the concrete bottom slabs were cracked, the flexural stiffness in the specimens BXL-A, BXL-B, and BXL-C were significantly decreased. And the flexural stiffness in the specimens BXL-A, BXL-B, and BXL-C were obviously different. The BXL-A specimen was the smallest, the BXL-B specimen was second, and the BXL-C specimen was the largest. For the BXL-D specimen, the flexural stiffness was hardly changed before up to ultimate load.

Fig. 12 showed the deflections in the specimens BXL-A, BXL-B, BXL-C, and BXL-D under the various loads 100 KN, 300 KN, 600 KN, and 800 KN. When the load was 100 KN, the deflections in the specimens BXL-A, BXL-B, BXL-C, and BXL-D were similar. When the load was 300KN, the deflections in the specimens BXL-A and BXL-D were larger than the other two specimens; when the load was 600 KN and 800 KN, the deflections in the BXL-A specimen were the largest.

The deflection values of specimens BXL-A, BXL-B, BXL-C, and BXL-D are shown in Table 4, where  $p_y$  is yield load,  $p_u$  is ultimate load,  $\delta_y$  is the deflection value caused by yield load,  $\delta_u$  is the deflection value caused by ultimate load,  $\delta_u/\delta_y$  is ductility factor.

The deflection values in the specimens BXL-A, BXL-B and BXL-C, which were similar, were 58 mm, 60 mm and 65 mm, respectively, and the corresponding yield loads were 550 KN, 620 KN and 820 KN. The yield load of the BXL-C specimen was largest, and was 49.1% larger than that of the BXL-A specimen, and was 32.3% larger than

Table 4 The deflection value of specimens

Specimens	$p_y$ (KN)	$p_u$ (KN)	$\delta_y$ (mm)	$\delta_u$ (mm)	$\delta_u / \delta_y$
BXL-A	550	822	58	485	8.82
BXL-B	620	930	60	415	6.92
BXL-C	820	1034	65	331	4.04
BXL-D	–	818	–	201	–

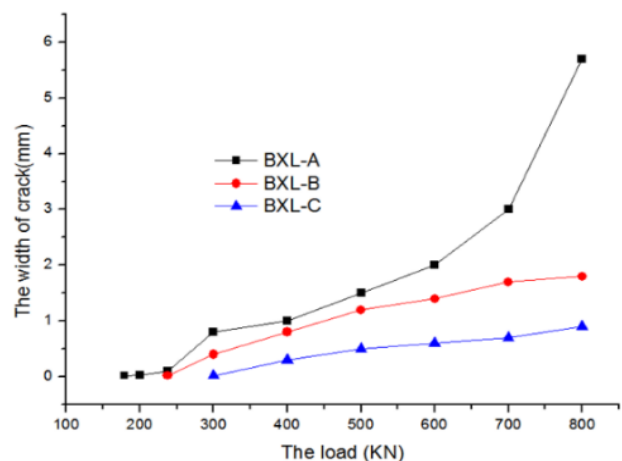


Fig. 13 Width of major crack with loading history

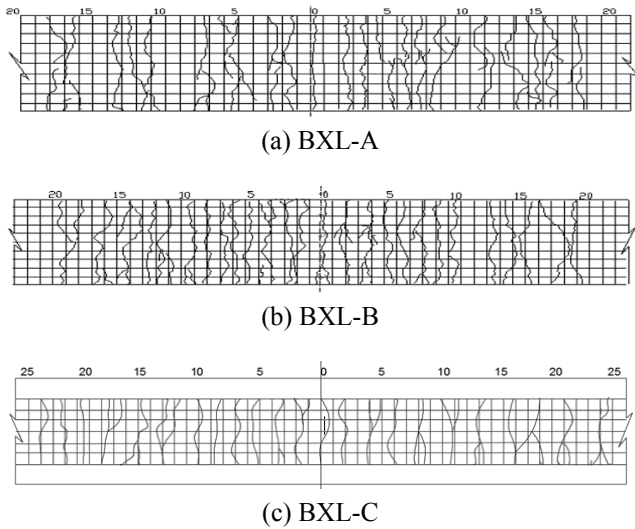


Fig. 14 Fractures on the concrete bottom slabs

that of the BXL-B specimen. So, the flexural stiffness of the BXL-C specimen was the largest. For the BXL-D specimen, because it was not yielded during the overall loading, the deflection values caused by yield load did not appear. So, the precise deflection values could not be gained by LVDT extensometer. However, Fig. 11 shows that, in the phase of the tension reinforcement yielding of the other three specimens, the flexural stiffness of the BXL-D specimen was larger than that of the specimens BXL-A and BXL-B, and was smaller than that of the BXL-C specimen.

Therefore, the conclusion can be drawn that the flexural stiffness of the optimized and upgraded composite box-girders with corrugated steel webs could observably be improved by the method that the concrete bottom slab was supported on the steel flanges.

In addition, the ductility factors of the specimens BXL-A, BXL-B and BXL-C were 8.82, 6.92 mm and 4.04 respectively. The ductility factor of the BXL-A specimen was greater than that of BXL-B and BXL-C.

#### 4.1.4 Crack resistance property in prestressed concrete composite box-girders with corrugated steel webs

If the concrete slab had cracked and the cracks had been enough wide, the water vapor, carbon dioxide and oxygen, etc., in the air would have been prone to contact the tense reinforcement in the concrete slabs and would have caused the tense reinforcement to be corroded. In order to avoid to the tense reinforcement corrosion, it is important to improve the crack resistance property of the prestressed concrete composite box-girders with corrugated steel webs.

The cracking loads of the BXL-A, BXL-B, and BXL-C specimen were 179 KN, 238 KN, and 300 KN, which were measured by the experiments. Therefore, the BXL-C specimen, on crack resistance property, is superior to the BXL-A specimen. In addition, because the concrete bottom slab of the BXL-D specimen was replaced by steel plate, the cracks will not appear on the bottom steel plate of the BXL-D specimen. So the BXL-D specimen, on the crack resistance property, was the most advantageous.

Fig. 13 showed the width of the major cracks on the concrete bottom of the specimens BXL-A, BXL-B, and BXL-C with the load history. The width of the major crack in the BXL-A specimen was considerably increased with load history, but the major cracks in the specimens BXL-B and BXL-C were eventually increased. In addition, the wide value of major crack of the BXL-A specimen was always bigger than that of the specimens BXL-B and BXL-C with load history.

Fig. 14 shows that the cracks were distributed on the concrete bottom slabs in the specimens BXL-A, BXL-B, and BXL-C. It can be observed that the cracks were distributed more uniformly on the concrete bottom slabs in the specimens BXL-C than in the other two specimens.

All these are illustrated that, on the crack resistance property, the BXL-C specimen is the best, the BXL-B specimen is the second, and the BXL-A specimen is the worst.

#### 4.1.5 Efficiency of prestressing introduced into box-girders with corrugated steel webs

Owing to the steel flanges, the efficiency of the prestressing introduced into the concrete bottom slab in the BXL-C specimen may be impacted. So it was necessary to research the efficiency of prestressing introduced into the prestressed concrete composite box-girders with corrugated webs. Because the prestressing tendons were not installed in the BXL-D specimen, the research was only focused on the specimens BXL-A, BXL-B and BXL-C.

In the course of experiment, the same effective prestressing, which was 3 MPa, was introduced into the concrete bottom slabs of the specimens BXL-A, BXL-B and BXL-C. The tensioned control stress on the end of the specimens BXL-A, BXL-B and BXL-C may be measured by the load cells laid on the specimen ends. The values of tensioned control stress are showed in the Table 5. After the effective prestressing value and the tensioned control stress value were obtained, the efficiency of the prestressing introduced into the concrete bottom slabs was easily

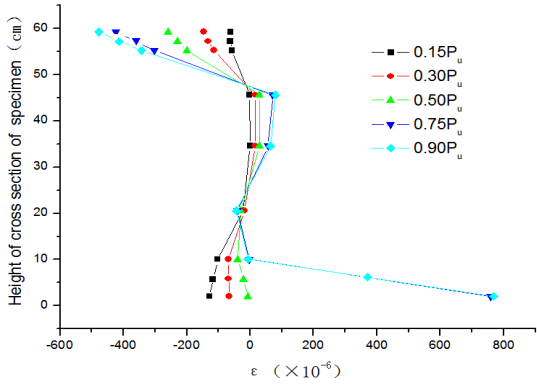
calculated by the formula  $\zeta = \frac{\sigma_y}{\sigma_c}$ , Where  $\zeta$  is the efficiency

of the prestressing introduced into the concrete bottom slabs;  $\sigma_y$  is the effective prestressing;  $\sigma_c$  is the tensioned control stress.

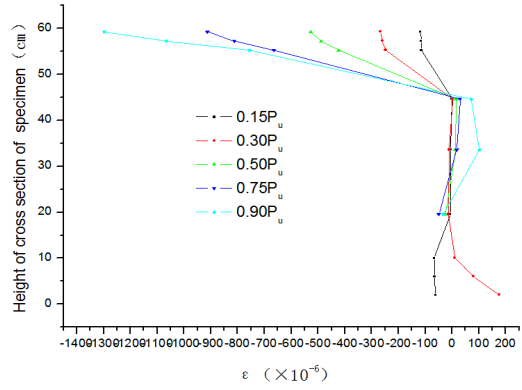
The efficiency of the prestressing introduced into the concrete bottom slabs of the test specimens BXL-A, BXL-B, and BXL-C were 93.75%, 88.24%, and 81.08%, respectively (as shown in the Table 5). The efficiency of the prestressing of the BXL-A specimen was highest, and that of the BXL-C specimen was lowest. Compared to BXL-A, the efficiency of the prestressing introduced into the

Table 5 Efficiency of prestressing introduced into the specimens

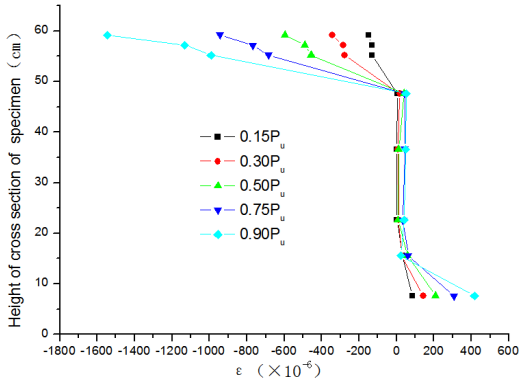
Specimens	BXL-A	BXL-B	BXL-C
Effective prestressing /MPa	3	3	3
Tensioned control stress /MPa	3.2	3.4	3.7
Efficiency of the prestressing introduced/%	93.75	88.24	81.08



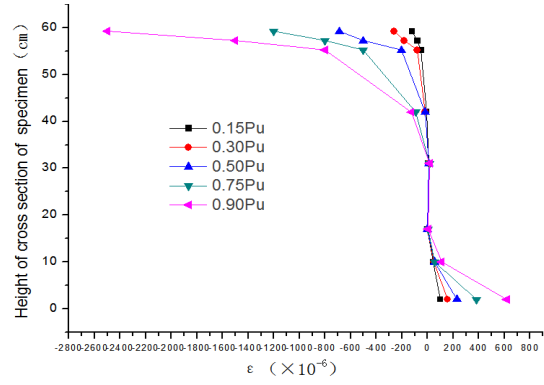
(a) BXL-A



(b) BXL-B

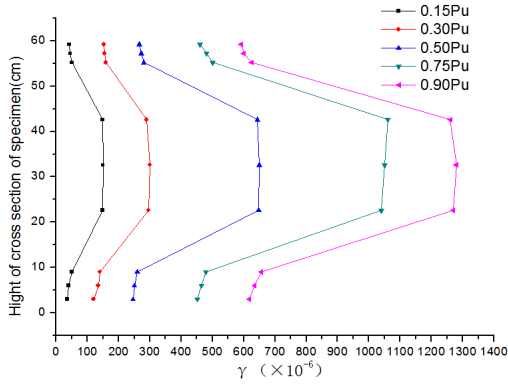


(c) BXL-C

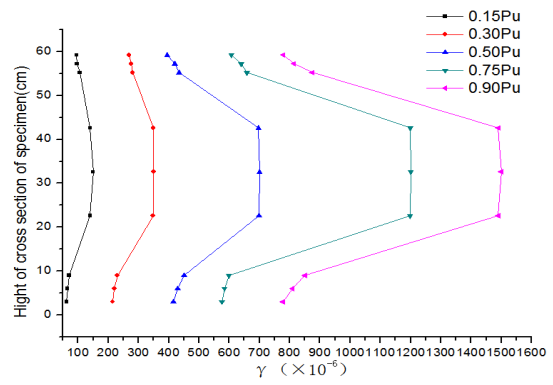


(d) BXL-D

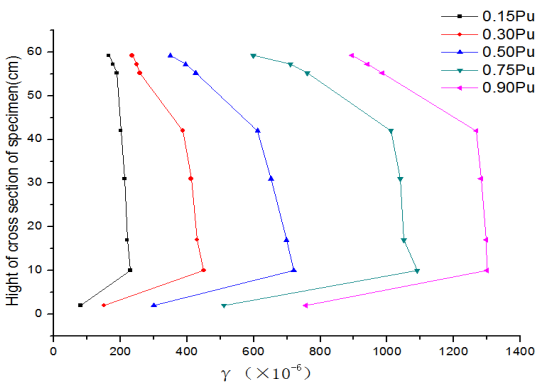
Fig. 15 Axial strain distributions along height of the cross section of specimens



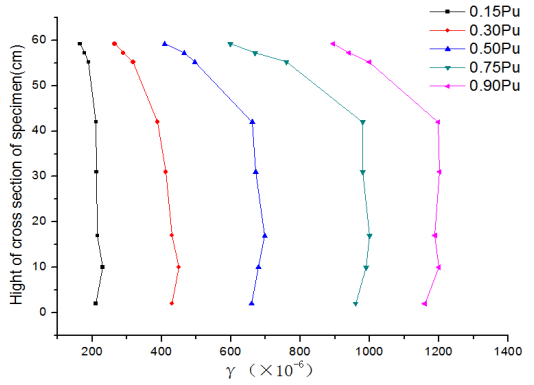
(a) BXL-A



(b) BXL-B



(c) BXL-C



(d) BXL-D

Fig. 16 Shearing strains distributions along height of cross section of specimens

concrete bottom slab of BXL-C was decreased by 13.51%. Therefore, the steel flanges have impacted the efficiency of the prestressing introduced into the concrete bottom slab of specimens. The steel flanges attached below the concrete bottom slab absorbed a part of prestressing which would have been applied on the concrete bottom slab, so the efficiency of the prestressing introduced into the concrete bottom slabs was reduced.

#### 4.1.6 Strains distribution on the cross section of the corrugated webs

- (a) The axial strains distributions along the height of the cross section of the corrugated webs.

Fig. 15 shows the axial strains distributed along the height of the cross section of the specimens BXL-A, BXL-B, BXL-C, and BXL-D, which were measured by strains gauges attached on the mid-span section of specimens under the different loads, which were  $0.15 p_u$ ,  $0.30 p_u$ ,  $0.50 p_u$ ,  $0.75 p_u$  and  $0.90 p_u$ . The axial strains on the corrugated webs were minimally changed and almost zero, while the axial strains on the top/bottom slabs were larger and increased with the load increasing (The phenomenon is described as the accordion effect (Chen *et al* 2015). The accordion effect can be clearly shown in all these specimens on Fig. 15. Therefore, the conclusion can be drawn that the flexural stiffness of the concrete top/bottom slabs was much greater than that of the corrugated webs, which was almost zero.

- (b) The shearing strains distributions along the height of the cross section of the corrugated webs.

Fig. 16 shows the shearing strains distributions along the height of the cross section of the specimens, which were measured by strains gauges attached on the mid-span section of specimens.

During the different loads, which were  $0.15 p_u$ ,  $0.30 p_u$ ,  $0.50 p_u$ ,  $0.75 p_u$  and  $0.90 p_u$ . The shearing strains on the top/bottom slabs were smaller, while the shearing strains on the corrugated webs were larger continued increasing as the load increased. It can be shown on Fig. 16 that the shearing stiffness on the corrugated webs was far greater than that on the top/bottom slabs.

#### 4.2 Impact of different shear connectors on the structure performances of the prestressed concrete composite box-girders with corrugated steel webs

In order to research the impact of the different shear connectors on structure performances, tests were conducted on the BXL-A specimen with shear studs and the BXL-B specimen with shear connectors PBL. The two specimens were fabricated with the same dimensions, materials, and environmental condition.

The specimens' end-slips, between the concrete top/bottom slabs and the steel flange, were measured by the guide rod extensometers installed at both ends of the specimens. The end slips of the BXL-A and BXL-B were initiated when the loads were 584 kN and 690 kN, And

when BXL-A and BXL-B failed, Their end slips reached the biggest values, which were 0.8 mm and 0.3 mm, respectively.

Impact of different shear connectors (PBL shear connectors and studs shear connectors) on behavior of the prestressed concrete composite box-girders with corrugated steel webs was investigated as following.

- (1) Impact of ultimate bearing capacity of the prestressed concrete composite box-girders with corrugated steel webs.

In the overall course of testing, the mechanical behaviors of the specimens BXL-A and BXL-B were very similar; the two specimens with PBL and studs shear connectors performed as a perfect material non - linearity, as shown in Fig. 11. However, the value of ultimate loads of specimens BXL-A and BXL-B, which were 822 KN and 930 KN (as shown in Table 4), respectively, were different. The value of BXL-B was 13.14% larger than one of the BXL-A. This illustrates that, compared to studs shear connectors, PBL shear connectors can improve the ultimate bearing capacities of prestressed concrete composite box-girders with corrugated steel webs.

- (2) Impact of flexural stiffness of the prestressed concrete composite box-girders with corrugated steel webs.

The load - displacement curves of BXL-A and BXL-B were similar, and there were two turning points on their curves (as shown in Fig. 11). Before the concrete bottom cracked, the curves of BXL-A and BXL-B almost coincided. After the concrete bottom cracked, the deflection of BXL-A was greater than that of BXL-B (as shown in Fig. 11). Table 5 shows that the deflection values caused by the yield load, on the specimens BXL-A and BXL-B, were 58 mm and 60 mm, and the deflection values caused by the ultimate load were 485 mm and 415 mm, and their ductility factor were 8.82 and 6.92, respectively. These illustrate that, in the elastic phase, the flexural stiffness of the girder was negligibly impacted by adopting the PBL or studs shear connectors, but in the plastic phase, the flexural stiffness of the girder was improved by adopting the PBL shear connectors.

- (3) Impact of different crack resistance property of the prestressed concrete composite box-girders with corrugated steel webs.

The crack load of the specimen BXL-A with studs shear connector was 179 KN, while the specimen BXL-B with PBL shear connector was 238 KN (as shown in Table 6). Compare to BXL-A, the crack load of BXL-B was increased by 33%. It shows that the crack resistance property of the specimen with the PBL shear connectors is superior to that of specimen with the studs shear connectors.

- (4) Impact of efficiency of prestressing introduced into the prestressed concrete composite box-girders with corrugated steel webs.

In order to research the impact of the different

shears connectors on the efficiency of prestressing introduced in the prestressed concrete composite box-girders with corrugated steel webs, the BXL-A specimen with studs shear connectors and the BXL-B specimen with PBL shear connectors were prestressed under the same conditions, including the same anchor system, the same strands and the same load time and speed, etc. Table 5 shows the efficiency of prestressing introduced into the specimens BXL-A and BXL-B were 93.75% and 88.24%, respectively. Compared to BXL-A, the efficiency of the prestressing introduced into the concrete bottom slab of BXL-B was decreased by 5.88%. Therefore, relative to the studs shear connector, the PBL shear connector reduced the efficiency of prestressing introduced in the prestressed concrete composite box-girders with corrugated steel webs.

## 5. Conclusions

In order to overcome some inherent drawbacks and improve its safety, in the study, the traditional prestressed concrete composite box-girders with corrugated steel webs was optimized and upgraded by two methods. The first method was to replace the concrete bottom slab with a steel plate and the second method was to support the concrete bottom slab on the steel flanges. Some behaviors of the optimized and upgraded girder were researched. In addition, impact of two types of shear connectors, PBL and studs, on behavior of the prestressed concrete composite box-girders with corrugated steel webs was quantitatively evaluated by test methods.

Some conclusions were drawn as follows:

- (1) The ultimate bearing capacities of the prestressed concrete composite box-girders with corrugated steel webs optimized and upgraded by supporting the concrete bottom slab on the steel flanges was greatly improved. But the ultimate bearing capacities of the one optimized and upgraded by replacing the concrete bottom slab with the steel plate was hardly improved.
- (2) The flexural stiffness of the prestressed concrete composite box-girders with corrugated steel webs optimized and upgraded by supporting the concrete bottom slab on the steel flanges, before the concrete bottom slab cracked, was hardly improved; however, after the concrete bottom slab cracked, it was noticeably improved. And the flexural stiffness of the one optimized and upgraded by replacing the concrete bottom slab with the steel plate was greatly improved.
- (3) In the crack resistance property, the prestressed concrete composite box-girders with corrugated steel webs optimized and upgraded by two methods (the first method was to replace the concrete bottom slab with a steel plate and the second method was to support the concrete bottom slab on the steel flanges) is greatly superior to the

traditional prestressed concrete composite box-girders with corrugated steel webs.

- (4) The efficiency of prestressing introduced into the prestressed concrete composite box-girders with corrugated steel webs optimized and upgraded by supporting the concrete bottom slab on the steel flanges was lower than the efficiency of introduced into traditional prestressed concrete composite box-girders with corrugated steel webs.
- (5) The ultimate bearing capacities of prestressed concrete composite box-girders with corrugated steel webs could be improved by using PBL shear connectors.
- (6) Before the concrete bottom slab cracked, the flexural stiffness of prestressed concrete composite box-girders with corrugated steel webs with the PBL shear connectors was similar to the one with the studs shear connectors. But after the concrete bottom cracked, the flexural stiffness of the girder with the PBL shear connectors was observably larger than one of the girder with the studs shear connectors.
- (7) In the crack resistance property, the prestressed concrete composite box-girders with corrugated steel webs with the PBL shear connectors was superior to the one with the studs shear connectors.
- (8) In the efficiency of prestressing introduced into box-girders with corrugated steel webs, the prestressed concrete composite box-girders with corrugated steel webs with the PBL shear connector was lower than the one with the studs shear connector.

## Acknowledgments

The financial support from the China Scholarship Council is gratefully appreciated.

## References

- Ahn, J.H., Lee, C.G., Won, J.H. and Kim, S.H. (2010), "Shear resistance of the perfobond-rib shear connector depending on concrete strength and rib arrangement", *J. Construct. Steel Res.*, **66**(10), 1295-1307.
- Barakat, S., Mansouri, A.A. and Altoubat, S. (2015), "Shear strength of steel beams with trapezoidal corrugated webs using regression analysis", *Steel Compos. Struct., Int. J.*, **18**(3), 757-773.
- Basher, M., Shanmugam, N.E. and Khalim, A. (2011), "Horizontally curved composite plate girders with trapezoidal corrugated webs", *J. Construct. Steel Res.*, **67**(6), 947-956.
- Chen, X.C., Ftk, A. and Bai, Z.Z. (2015), "Flexural ductility of reinforced and prestressed concrete sections with corrugated steel webs", *Comput. Concrete, Int. J.*, **16**(4), 625-642.
- Ding, Y., Jiang, K.B. and Liu, Y.W. (2012), "Nonlinear analysis for PC box-girder with corrugated steel webs under pure torsion", *Thin-Wall. Struct.*, **51**(2), 167-173.
- He, J., Liu, Y., Chen, A. and Yoda, T. (2012), "Mechanical behavior and analysis of composite bridges with corrugated steel webs: State-of-the-art", *Int. J. Steel Struct.*, **12**(3), 321-338.

- He, J., Liu, Y.Q., Xu, X.Q. and Li, L.B. (2014), "Loading capacity evaluation of composite box girder with corrugated webs and steel tube slab", *Struct. Eng. Mech., Int. J.*, **50**(4), 501-524.
- Huang, Q.W. and Chen, B.C. (2016), "Trial design for concrete arch bridge with corrugated steel web", *J. Harbin Inst. Technol.*, **23**(6), 16-24. [In Chinese]
- Jung, K.H., Kim, K.S., Sim, C.W. and Kim, J.H.J. (2011), "Verification of incremental launching construction safety for the Ilsun Bridge, the world's longest and widest prestressed concrete box girder with corrugated steel web section", *J. Bridge Eng.*, **3**(5), 453-460.
- Kim, K.S., Lee, D.H., Choi, S.M., Choi, Y.H. and Jung, S.H. (2011), "Flexural behavior of prestressed composite beams with corrugated webs: Part I. Development and analysis", *Compos. Part B Eng.*, **42**(6), 1603-1611.
- Lee, D.H., Oh, J.Y., Kang, H., Kim, K.S., Kim, H.J. and Kim, H.Y. (2015), "Structural performance of prestressed composite girders with corrugated steel plate webs", *J. Construct. Steel Res.*, **104**(7), 9-21.
- Li, L., Xiao, X. and Liu, Q. (2012), "Study on the residual flexural capacity of composite box girders with corrugated steel webs after fatigue damage", *China Civil Eng. J.*, **45**(7), 111-119.
- Nie, J., Tao, M.X., Wu, L., Nie, X. and Lei, F. (2012), "Advance of research on steel - concrete composite bridge", *China Civil Eng. J.*, **45**(6), 110-122.
- Sause, R., Abbas, H.H., Driver, R.G., Anami, K. and Fisher, J.W. (2015), "Fatigue life of girders with trapezoidal corrugated webs", *J. Struct. Eng.*, **132**(7), 1070-1078.
- Song, S.D., Zhu, B., Chen, K.J. and Xiang, B.S. (2014), "Mechanical performance research on the box girder with corrugated steel webs without considering slippage", *J. Railway Eng. Soc.*, **31**(6), 50-55.
- Yong, D., Kebin, J., Fei, S. and Anzhong, D. (2013), "Experimental study on ultimate torsional strength of PC composite box-girder with corrugated steel Webs under pure torsion", *Struct. Eng. Mech., Int. J.*, **46**(4), 519-531.